

Spatiotemporal Bifurcation Phenomena with Temporal Period Doubling: Patterns in Vibrated Sand

Shankar C. Venkataramani¹ and Edward Ott²

¹*James Franck Institute, University of Chicago, Chicago, Illinois 60637*

²*University of Maryland, College Park, Maryland 20742*

(Received 30 September 1997)

This paper examines the consequences of the interaction between temporal period doubling and spatial pattern formation. We propose a simple discrete time, spatially continuous system, where the discrete time dynamics incorporates period doubling and the spatial operator imposes patterning at a preferred length scale. We find that this model displays a variety of bifurcations between different spatiotemporal states, and these bifurcations are generic in that they do not depend on the details of the model. The results from our simple model bear remarkable similarities with recent experiments on a vertically vibrated granular layer. [S0031-9007(98)05842-6]

PACS numbers: 05.45.+b, 46.10.+z, 47.54.+r, 81.05.Rm

In this paper we examine the consequences of the interaction between temporal period doubling and spatial pattern formation. Our study was motivated originally by experiments [1–3] in which the authors observed the formation of a variety of two-dimensional patterns in a vertically vibrated thin granular layer [4]. These patterns are the analog of Faraday waves in vibrated fluids. In the experiments in [1–3], the granular layer is on a horizontal plate with an upper free surface and the plate is vertically vibrated. Varying the amplitude and the frequency f_0 of the sinusoidal vibration leads to transitions between the various patterned states. For example, in Ref. [1], holding f_0 fixed and increasing the oscillation amplitude, the following sequence of states was observed: a uniform flat state oscillating at f_0 ; a stripe pattern oscillating at $f_0/2$ (i.e., the period of the pattern oscillation is double the vibrational period); a hexagonal pattern, also at $f_0/2$; two flat domains separated by a “kink” with each domain oscillating at $f_0/2$ but with each in one of the two possible temporal $f_0/2$ phases of oscillation; competing square and stripe patterns at $f_0/4$ (i.e., a further period doubling has occurred); $f_0/4$ hexagonal patterns; and, at higher driving, patterns disordered in space and time. [See Figs. 1(a)–1(f) of Ref. [1].] In Refs. [2] and [3], additional phenomena are reported, the most interesting of which is the presence of localized, solitary structures oscillating at $f_0/2$, which the authors call *oscillons*.

As the authors remark in [3], these experiments provide a challenge to theory. Unlike in a fluid flow, where the equations of hydrodynamics provide an adequate description of the pattern formation, there exist no corresponding equations describing the flow of granular materials [5,6]. The only direct, first-principle, approach to studying the dynamics of granular materials with many interacting particles has been molecular-dynamics-type numerical simulations. Such molecular dynamics simulations of spheres on a vibrating plate reproduce the experimentally observed phenomena [7]. Another useful approach to this problem

has been to model the dynamics of the vibrated granular layer using heuristic or hydrodynamics-type equations [8].

Because of the current lack of physical understanding of dynamics of granular media [5], and the possibility that there exist no local equations describing granular flow [6], it seems that one reasonable approach to study this phenomenon is to formulate a simple model incorporating what one expects are the essential qualitative features of the phenomena observed. To the extent that the model is free of physics specific to the experiment, we can regard the experimentally observed features reproduced by the model as universal. This approach would enable one to identify the key features that lead to the observed experimental behavior, and it will explain why models with different assumptions on the underlying physics can yield results in qualitative agreement with the experiments.

In [1], the authors argue that the various patterns they observe are produced by the interaction between a temporal period doubling sequence and an instability that produces standing waves on the surface of the layer. These are the two essential features we choose to incorporate into our model, viz. temporal period doubling and patterning at a preferred spatial scale. Our model is as follows. We consider a scalar field $\xi_n(\mathbf{x})$ at discrete integer valued times n which we think of as representing the height of the granular layer at position \mathbf{x} , where \mathbf{x} is a continuous two-dimensional spatial variable. To advance $\xi_n(\mathbf{x})$ forward one time period, we first apply a one-dimensional map M to ξ_n at each point in space,

$$\xi'_n(\mathbf{x}) = \mathbf{M}(\xi_n(\mathbf{x}), \mathbf{r}), \quad (1)$$

where r is a parameter of the chosen map function. We shall be particularly interested in varying r through period doublings of the map M . Next, we augment this nonlinear discrete time dynamics with a linear spatial operator \mathcal{L} which couples the dynamics of nearby \mathbf{x} locations,

$$\xi_{n+1}(\mathbf{x}) = \mathcal{L}[\xi'_n(\mathbf{x})]. \quad (2)$$

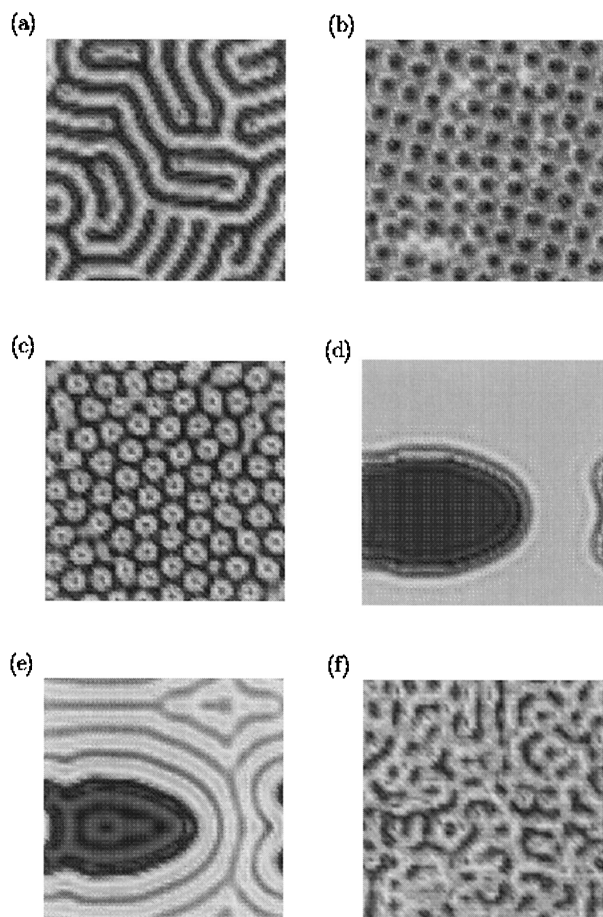


FIG. 1. Extended patterns obtained numerically in our model. (a) Period-2 stripes at $r = 1.9, (k_c/k_0)^2 = 5$. (b) Period-2 squares at $r = 1.9, (k_c/k_0)^2 = 1.5$. (c) Period-2 hexagons at $r = 2.05, (k_c/k_0)^2 = 2.6$. (d) Period-2 flat state with a kink at $r = 2.4, (k_c/k_0)^2 = 5$ (the kink is the border region between the high ξ and the low ξ areas). (e) Period-4 stripes at $r = 2.7, (k_c/k_0)^2 = 5.0$. (f) Disorder at $r = 3.2, (k_c/k_0)^2 = 5$.

Letting $\bar{\xi}_n(\mathbf{k})$ denote the spatial Fourier transform of $\xi_n(\mathbf{x})$ and setting $\bar{\mathcal{L}}(\mathbf{k}) = \mathbf{f}(\mathbf{k})$, we have

$$\bar{\xi}_{n+1}(\mathbf{k}) = \mathbf{f}(\mathbf{k})\bar{\xi}_n'(\mathbf{k}). \quad (3)$$

If we imagine that the patterns on the surface of the vibrated layer are a superposition of standing waves, the quantity $\log |f(\mathbf{k})|$ is the growth rate for the amplitude of the standing wave with wave vector \mathbf{k} between two collisions with the plate. Assuming isotropy, we henceforth write f as a function of $k = |\mathbf{k}|$. We assume that $f(k)$ is real and we incorporate spatial patterning at a preferred scale k_0^{-1} by taking $|f(k)|$ to have a peak at $k = k_0$, $|f(k_0)| > 1$, after which $|f(k)|$ decreases with increasing k , becoming small [$|f(k)| \ll 1$] at large k .

For most of the numerical results in this paper, we use the map

$$M(\xi, r) = r \exp[-(\xi - 1)^2/2], \quad (4)$$

and we choose $f(k) = \phi(k) \exp[\gamma(k)]$, where

$$\gamma(k) = \frac{1}{2} \left(\frac{k}{k_0} \right)^2 \left[1 - \frac{1}{2} \left(\frac{k}{k_0} \right)^2 \right], \quad (5)$$

$$\phi(k) = \text{sgn}(k_c^2 - k^2). \quad (6)$$

The map in Eq. (4) is similar to the logistic map but it has the advantage that orbits cannot run away to infinity. All of the period doublings in this map are supercritical. The form of the growth rate $\gamma(k) = \log |f(k)|$ in Eq. (5) is a simple choice for an even function that is zero at $k = 0$, has a peak at $k = k_0$, and is negative for large k . The presence of the factor $\phi(k)$ allows f to change sign with k , and its form in Eq. (6) is a simple (rather arbitrary) choice for a function that is even in k and changes sign as we change k . The factor ϕ introduces a second length scale in our model [9] and the model has two dimensionless parameters, r and k_c/k_0 , which, we numerically find, roughly play roles analogous to the dimensionless acceleration Γ and the frequency f_0 of the drive in the experiment. In order to keep $f(k_0) > 0$, we will take $k_c > k_0$. As will become clear from the theory, the important bifurcation phenomena are independent of the specific choices in (4)–(6).

We emphasize that we view Eqs. (1)–(6) as a minimalist model and that several obvious generalizations immediately suggest themselves [e.g., complex f in (3), a two-dimensional (or higher) map replacing the one-dimensional map (1), etc.]. Our point is that even this simple representation is rich enough to display many of the experimentally observed effects and that certain of these effects can be regarded as physics independent and universal for systems in which patterning and period doubling interact.

Figures 1(a)–1(f) show numerical results from our model as r and k_c are changed. These pictures are qualitatively similar to those in Ref. [1]. We regard as particularly significant the fact that, in our model, as we increase r , the bifurcation sequence is a period-1 flat state bifurcating to give a period-2 pattern which then becomes a period-2 flat state and, eventually, a period-4 pattern. Thus, *with an increase of the parameter, the period-2 and period-4 patterns are separated by a period-2 flat state*. This basic sequence, also observed in the experiment, is universal in that it does not depend on the details of the model. In particular, it is present even with $\phi(k)$ removed, i.e., $f(k) = \exp[\gamma(k)]$.

The separation of the patterned period-2 and patterned period-4 states by a period-2 homogeneous state can be understood as a result of the following elementary stability analysis. For a given value of r , let the map $M(\xi, r)$ have a stable period- p periodic orbit $\xi_1, \xi_2, \dots, \xi_p$. Then, $M(\xi_p, r) = \xi_{p+1} = \xi_1$. The stability index of the periodic orbit is given by $\lambda_p(r) = N(\xi_1)N(\xi_2) \cdots N(\xi_p)$ with $N(\xi) = \partial M(\xi, r)/\partial \xi$. The orbit being stable implies that $|\lambda_p(r)| < 1$.

We now consider the stability of the sequence of spatially homogeneous states $\xi_n(\mathbf{x}) = \xi_i$ to small perturbations, so that $\xi_n(\mathbf{x}) = \xi_n + \delta \xi_n(\mathbf{x})$. Equation (1) yields $\delta \xi_{n+1}'(\mathbf{x}) = \mathbf{N}(\xi_n) \delta \xi_n(\mathbf{x})$. Equation (2) yields $\delta \xi_{n+1}(\mathbf{k}) = \mathbf{N}(\xi_n) \mathbf{f}(\mathbf{k}) \delta \xi_n(\mathbf{k})$. After p iterations, we have $\delta \xi_{n+p}(\mathbf{k}) = \lambda_p(\mathbf{r}) [\mathbf{f}(\mathbf{k})]^p \delta \xi_n(\mathbf{k})$. The instability of a $k = k_0$ pattern results for $|\lambda_p(r) [f(k_0)]^p| > 1$. Therefore, the period- p spatially homogeneous states are stable to spatially varying perturbations if $|\lambda_p(r) [f(k_0)]^p| < 1$, are unstable to a period- p spatially varying state if $\lambda_p(r) [f(k_0)]^p > 1$, and are unstable to a period- $2p$ pattern if $\lambda_p(r) [f(k_0)]^p < -1$.

Figure 2(a) is a bifurcation diagram for a generic map $M(\xi, r)$ that undergoes period doubling and Fig. 2(b) is the stability index for attracting periodic orbits (or fixed points). At $r = r_a$, the period-1 orbit of the map is superstable so that $\lambda_1(r_a) = 0$. As we increase r , at $r = r_c$, $\lambda_1(r_c) = -1$ and the map M undergoes a period doubling. On further increasing r , the period-2 orbit becomes superstable at $r = r_e$ so that $\lambda_2(r_e) = 0$. Because $f(k_0) > 1$, it is clear that there exists a r_b with $r_a < r_b < r_c$ such that $\lambda_1(r_b) f(k_0) = -1$. Therefore, the period-1 homogeneous state becomes unstable to a period-2 pattern at $r = r_b$. Also, there exists an r_d with $r_c < r_d < r_e$ such that $\lambda_2(r_d) f^2(k_0) = 1$. At this point, the period-2 homogeneous state becomes stable. On further increasing r , there exists a parameter value r_f with $r_f > r_e$ such that $\lambda_2(r_f) f^2(k_0) = -1$. At this value of r , the period-2 homogeneous state becomes unstable to a period-4 pattern.

The elementary stability considerations above give us the values of the parameter r at which there are bifurcations between flat states and patterned states. These considerations are strictly valid only close to the onset of the pattern formation. We have used a truncated modal

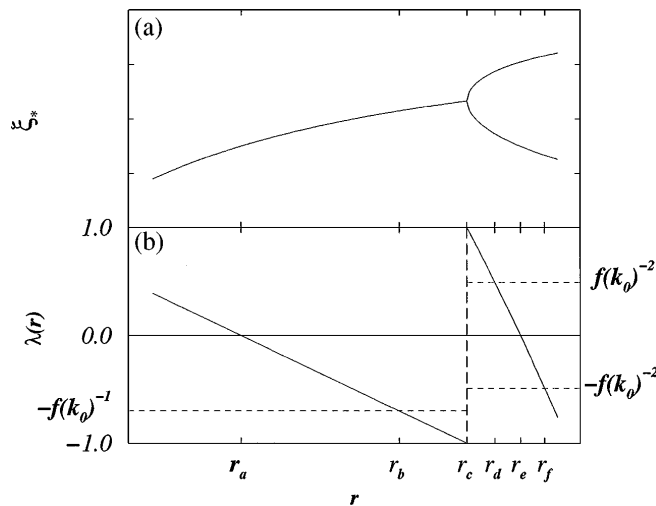


FIG. 2. (a) Schematic bifurcation diagram near a period doubling. (b) The stability index $\lambda(r)$ for the stable periodic (fixed) points.

expansion to obtain finite amplitude stripe, square, and hexagon solutions in the nonlinear regime away from the onset. With this approach, we can determine the patterns selected away from onset, and we will report these results in a future publication [10].

Figure 3(a) shows the approximate locations in the two parameter space $[r, (k_c/k_0)]$ of the various spatiotemporal behaviors numerically exhibited by our model. The phases in the figure correspond to states that evolve from starting at a small initial perturbation about a homogeneous state. (If, on the other hand, we follow large amplitude states by slow parameter change, then we find that some of the transitions that are nonhysteretic in the experiment show substantial hysteresis in the model.) We note that, if we crudely identify r with the experimental dimensionless acceleration Γ and k_c/k_0 with the experimental frequency f_0 , then there is striking qualitative agreement between the phase diagram obtained numerically from our model, Fig. 3(a), and the experimental phase diagram, Fig. 3(b).

The bifurcations for the map in (4) are all supercritical. The map $M(\xi, r) = -(r\xi + \xi^3) \exp(-\xi^2/2)$ has a

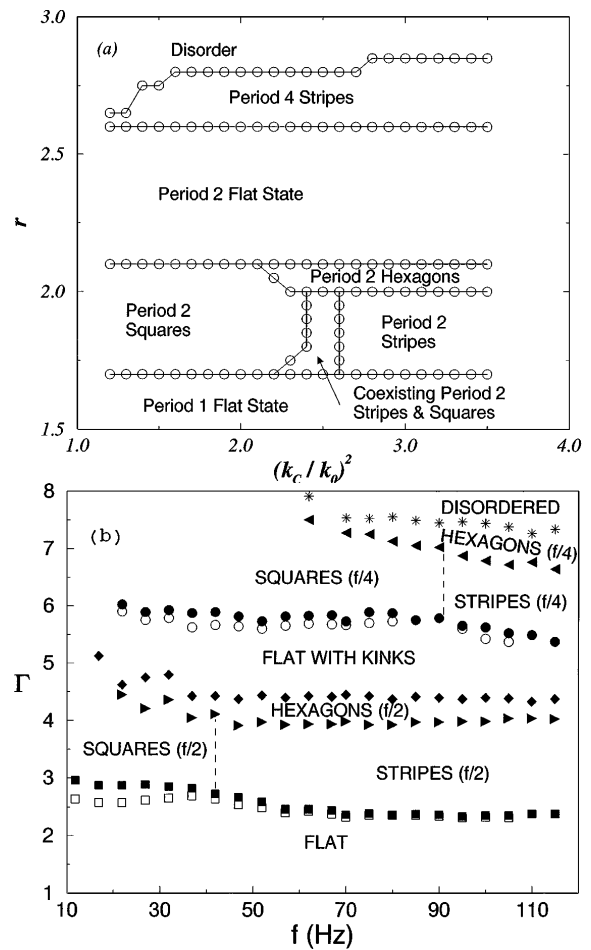


FIG. 3. (a) Phase diagram showing the various stable patterns seen in numerical simulations with the model Eqs. (1)–(6). (b) Experimental phase diagram from Refs. [1,3].

subcritical period doubling from period 1. With this map used in place of Eq. (4), we see period-2 localized states in the regime where the period-1 flat state is stable. These structures are similar to the oscillons seen in the experiments [2,3]. Figure 4(a) shows two oscillons in opposite temporal phases and Fig. 4(b) shows a bound state of several close oscillons. (We note that Tsimring and Aranson [8] also obtain oscillons, and their model also has a subcritical period doubling. It thus appears that subcriticality may be the key to the oscillon phenomenon.) The oscillons that we find numerically in our model are stable in the parameter range of the hysteretic transition from the period-1 flat state to the period-2 squares, as in the experiments.

We now offer some further comments on the meaning of universality for our model: First, we note that by separating the temporal dynamics [Eq. (1)] and the spatial coupling [Eq. (2)], our model has a special structure that is not, in general, present in physical situations. However, the individual qualitative spatiotemporal bifurcations we find are generic in that they persist [10] under changes that “mix” the temporal and spatial dynamics. This genericity implies that these bifurcations may be physically observable in systems other than vibrated granular layers [10]. As a second point, we note that a designation of a phenomenon as “generic” or “universal” does not imply that it always occurs [e.g., for a smooth map $M(x, r)$ a single period doubling does not necessarily guarantee the occurrence of a full period doubling cascade]. For example, in the case of Faraday waves on a vertically vibrated fluid layer, a period doubled homogeneous state is ruled out by incompressibility. Thus, for such a system the bifurcation at $r = r_d$ cannot occur. (Similarly, different choices of M and \mathcal{L} in (1) and (2) may produce phase diagrams that differ somewhat from Fig. 3.)

In conclusion, we remark that the spirit of our model is similar to that of other generic models of spatiotemporal dynamics [11], and may be regarded as lying between continuous time/continuous space models (e.g., the Swift-Hohenberg and the complex Ginzburg-Landau equations) and coupled map lattice models [12,13]. Our choice of

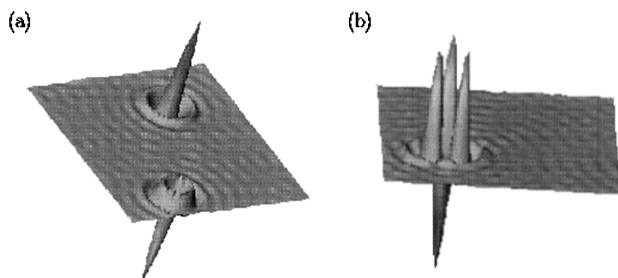


FIG. 4. Localized states obtained using the map with subcritical bifurcations. (a) Two oscillons out of phase [$r = 0.65, (k_c/k_0)^2 = 1.7$]. (b) A bound state with coordination number 3 [$r = 0.55, (k_c/k_0)^2 = 1.7$].

discrete time provides the simplest possible description of temporal period doubling, while our choice of continuous space allows spatial patterns unconstrained by an imposed grid [14]. Further results from this model will be reported in Ref. [10].

We thank Greg Huber, Heinrich Jaeger, Paul Umbanhowar, and Harry Swinney for useful discussions. The work of S.C.V. was supported by NSF DMR 9415604 and that of E.O. was supported by the Office of Naval Research (Physics).

-
- [1] F. Melo, P.B. Umbanhowar, and H.L. Swinney, *Phys. Rev. Lett.* **75**, 3838 (1995).
 - [2] P.B. Umbanhowar, F. Melo, and H.L. Swinney, *Nature (London)* **382**, 793 (1996).
 - [3] P.B. Umbanhowar, F. Melo, and H.L. Swinney, “Periodic, Aperiodic and Transient Patterns in Vibrated Granular Layers” (to be published).
 - [4] For other experiments exhibiting phenomena in vertically vibrated granular layers, see the following: T. Metcalf, J.B. Knight, and H.M. Jaeger, *Physica (Amsterdam)* **236A**, 202 (1997); F. Melo, P.B. Umbanhowar, and H.L. Swinney, *Phys. Rev. Lett.* **72**, 172 (1994); H.K. Pak and R.P. Behringer, *Phys. Rev. Lett.* **71**, 1832 (1993); C. Larouche, S. Douady, and S. Fauve, *J. Phys. (France)* **50**, 699 (1989); M. Faraday, *Philos. Trans. R. Soc. London* **52**, 299 (1831).
 - [5] H.M. Jaeger, S.R. Nagel, and R.P. Behringer, *Rev. Mod. Phys.* **68**, 1258 (1996).
 - [6] L.P. Kadanoff, “Built Upon Sand: Theoretical Ideas Inspired by the Flow of Granular materials” (to be published).
 - [7] C. Bizon *et al.*, *Phys. Rev. Lett.* **80**, 57 (1998).
 - [8] L.S. Tsimring and I.S. Aranson, *Phys. Rev. Lett.* **79**, 213 (1997); T. Shinbrot, *Nature (London)* **389**, 574 (1997); E. Cerda, F. Melo, and S. Rica, *Phys. Rev. Lett.* **79**, 4570 (1997); D. Rothman (to be published); J. Eggers and H. Riecke (private communication).
 - [9] R. Lifshitz and D.M. Petrich, *Phys. Rev. Lett.* **79**, 1261 (1997). The authors modify the Swift-Hohenberg equation by introducing a second length scale, and this leads to patterns besides stripes.
 - [10] S.C. Venkataramani and E. Ott (to be published). Among other things, in this longer paper, we discuss specific candidate systems besides vibrated granular layers, where the generic bifurcation phenomena found in our model may be present.
 - [11] M.C. Cross and P.C. Hohenberg, *Rev. Mod. Phys.* **65**, 854 (1993).
 - [12] See, e.g., K. Kaneko, *Chaos* **2**, 279 (1992). This issue of *Chaos* focuses on the subject of coupled map lattices.
 - [13] Another in-between case is provided by coupled ordinary differential equations on a spatial lattice, e.g., D.K. Umberger, C. Grebogi, E. Ott, and B. Afreyan, *Phys. Rev. A* **39**, 4835 (1989).
 - [14] In numerical solutions of (1) and (2) a spatial grid is used, but the spacing between the grid points is small compared to the characteristic scale k_0^{-1} .